HHS Public Access

Author manuscript

Oncogene. Author manuscript; available in PMC 2021 December 30.

Published in final edited form as:

Oncogene. 2021 August ; 40(32): 5095–5104. doi:10.1038/s41388-021-01843-0.

Generation of human embryonic stem cell models to exploit the *EWSR1-CREB* fusion promiscuity as a common pathway of transformation in human tumors

Fabio Vanoli[1], **Brigita Meskauskaite**[1], **Laurie Herviou**[1], **William Mallen**[1], **Yun-Shao Sung**[1], **Yumi Fujisawa**[1], **Lei Zhang**[1], **Steven Simon**[1], **Danwei Huangfu**[2], **Maria Jasin**[2], **Cristina R Antonescu**[1]

[1]Department of Pathology, Memorial Sloan Kettering Cancer Center, New York, NY, USA

[2]Developmental Biology Program, Memorial Sloan Kettering Cancer Center, New York, NY, USA

Abstract

Chromosomal translocations constitute driver mutations in solid tumors and leukemias. The mechanisms of how related or even identical gene fusions drive the pathogenesis of various tumor types remain elusive. One remarkable example is the presence of *EWSR1* fusions with *CREB1* and *ATF1,* members of the CREB family of transcription factors, in a variety of sarcomas, carcinomas and mesotheliomas. To address this, we have developed *in vitro* models of oncogenic fusions, in particular, *EWSR1-CREB1* and *EWSR1-ATF1,* in human embryonic stem (hES) cells, which are capable of multipotent differentiation, using CRISPR-Cas9 technology and HDR together with conditional fusion gene expression that allows investigation into the early steps of cellular transformation. We show that expression of *EWSR1-CREB1/ATF1* fusion in hES cells recapitulates the core gene signatures, respectively, of angiomatoid fibrous histiocytoma (AFH) and gastrointestinal clear cell sarcoma (GI-CCS), although both fusions lead to cell lethality. Conversely, expression of the fusions in hES cells differentiated to mesenchymal progenitors is compatible with prolonged viability while maintaining the core gene signatures. Moreover, in the context of a mesenchymal lineage, the proliferation of cells expressing the *EWSR1-CREB1* fusion is further extended by deletion of the tumor suppressor *TP53*. We expect the generation of isogenic lines carrying oncogenic fusions in various cell lineages to expand our general understanding of how those single genetic events drive tumorigenesis while providing valuable resources for drug discovery.

Materials & Correspondence Maria Jasin, PhD: m-jasin@ski.mskcc.org and Cristina R. Antonescu, MD: antonesc@mskcc.org.

Author contributions.

F.V., M.J. and C.R.A. conceived the project, designed experiments, and supervised the research. F.V., B.M, L.H, W.M, Y.F., S.S. and L.Z. performed experiments. Y.S.S. analyzed the Affymetrix U133A and the RNA sequencing data. D.H. provided reagents. F.V., M.J. and C.R.A. wrote the paper with input from D.H.

Competing interests.

The authors declare no competing interests.

Keywords

EWSR1; CREB1; ATF1; CRISPR-Cas9; sarcoma; angiomatoid fibrous histiocytoma; clear cell sarcoma; hES cells; hES-MP cells

INTRODUCTION

Gene fusions involving *EWSR1* with members of the cAMP response element binding protein (CREB) family, in particular *ATF1* and *CREB1*, are the main oncogenic drivers of several tumors, including angiomatoid fibrous histiocytoma (AFH), soft tissue and gastrointestinal clear cell sarcoma (CCS), young adult mesothelioma and hyalinizing clear cell carcinoma [1–6]. Although *CREB1* and *ATF1* are found as gene partners within the same tumor type, there is a propensity for the *EWSR1-CREB1* fusion to occur in AFH and *EWSR1-ATF1* in soft tissue CCS. An exception is the gastrointestinal CCS (GI-CCS) with the 2 fusions occurring with similar prevalence.

AFH is a mesenchymal neoplasm of borderline malignant potential, typically occurring in the superficial soft tissues of children and adolescents [1, 7]. Soft tissue CCS is a high-grade sarcoma prevalently found in the deep soft tissues of young adults and shows melanocytic differentiation, being positive for MITF and MelanA markers, as well as SOX10 [2, 8]. By contrast, GI-CCS is an aggressive malignant neoplasm that occurs in the gastric or small bowel wall of young adults lacking melanocytic differentiation [3].

Analysis of the etiology of these *EWSR1-CREB* family translocation-associated tumors and their therapeutic vulnerabilities has been hindered by the paucity of disease models, in particular human cell lines expressing the fusions [9]. The development of genome editing techniques has facilitated the generation of chromosomal translocations in human cell lines [10]. Double strand breaks (DSBs) are introduced into the two genes involved in the fusion, and non-homologous end joinin of the two DSBs results in a chromosomal translocation. However, the process is inefficient, since cells generally repair DSBs without translocation and the recovery of clones harboring the translocation is difficult if the fusion does not induce cellular transformation or impairs cell proliferation.

In this study we developed an approach combining CRISPR-Cas9 technology and homology-directed repair (HDR), which allows the selection of translocation-positive clones and conditional expression of the fusion. Using this strategy we isolated clones harboring the *EWSR1-WT1* translocation, the genetic hallmark of desmoplastic small round cell tumor (DSRCT), in human embryonic stem-derived mesenchymal progenitor (hES-MP) cells [11] even if the limited number of passages of the non-immortalized hES-MP cells hampered further investigation on the role of the fusion in sarcomagenesis.

To surmount this limitation, we propose a strategy to generate chromosomal translocations in human embryonic stem (hES) cells that grow almost indefinitely and can differentiate into a variety of cell types. We show that hES cells harboring a chromosomal translocation can be differentiated into hES-MP cells allowing the characterization of the fusion and its role in sarcomagenesis upon conditional expression. Our *in vitro* models of *EWSR1-CREB1* and

EWSR1-ATF1 fusions recapitulate the transcriptional profiles found in human tumors with these gene fusions. As the spectrum of tumors driven by these fusions include mesenchymal (AFH and GI-CCS), neuroectodermal (CCS), and epithelial (carcinoma, mesothelioma) lineages, we consider hES cells an optimal system for modeling translocation.

RESULTS

Human AFH and CCS driven by *EWSR1-CREB* fusions have distinct gene expression profile.

Most cases of AFH (90%) harbor a t(2;22)(q34;q12) translocation (Fig. 1A), with a resulting *EWSR1-CREB1* transcript that fuses *EWSR1* exons 1–7 with *CREB1* exons 7–8 [1, 7]. We have previously defined the gene expression profile of human AFH showing that the top upregulated genes are serum and glucocorticoid-regulated kinase 1 (*SGK1*), matrix-remodeling-associated protein 5 (*MXRA5*), and cathepsin B precursor (*CTSB*) [1]. This expression signature, designated as the 'AFH core gene signature', was re-analyzed and confirmed as part of this study compared to a large number of sarcomas and normal tissues available on the same Affymetrix U133A array platform (Fig. 1B).

The genetic hallmark of soft tissue CCS is a t(12;22)(q13;q12) (Fig. 1C), resulting in an *EWSR1-ATF1* fusion, although rare examples of cases with *EWSR1-CREB1* fusions have also been documented [8, 12]. Tumors with *EWSR1-ATF1* translocation express multiple isoforms. The most common transcripts include *EWSR1* exons 1–8 or 1–7 fused to *ATF1* exons 4–7 or 5–7, respectively [2, 8]. Other less common variants have been identified, including an out-of-frame fusion, presumably resulting from alternative splicing (*EWSR1* exons 1–7, *ATF1* exons 4–7), of questionable oncogenic potential [8]. The soft tissue CCS core gene signature includes several melanocytic markers (*MITF* and *PMEL*), the transcription factor *SOX10*, the amino-acid transporter *SLC7A5,* and the phosphatase *DUSP4* [1] (Fig. 1D).

The above core gene signatures were then tested in two additional AFH tumors expressing the *EWSR1-CREB1* fusion (AFH31.2 and AFH61, Fig. 1E), and two additional soft tissue CCS tumors expressing the in-frame *EWSR1*(ex8)-*ATF1*(ex4) fusion (1T and 22T; Fig. 1F). By quantitative RT-PCR (qRT-PCR), *SGK1* and *MXRA5* were confirmed to be upregulated in the AFH tumors but not the CCS tumors (Fig. 1E, F). In contrast, *PMEL* and *SOX10* were upregulated in the CCS tumors compared to the AFH tumors while *MITF* was only expressed in CCS but not AFH (Fig. 1F and S1A). *SLC7A5* and *DUSP4* genes were substantially upregulated in the CCS tumors, but also in one of the AFH tumors (AFH61) (Fig. 1E, 1F).

GI-CCS harbors an *EWSR1-CREB1* fusion in more than half of the cases, with the remaining showing *EWSR1-ATF1* fusion [3, 13]. The data on GI-CCS transcriptional profiling remains limited, with one case harboring an *EWSR1-CREB1* fusion previously analyzed by our group with *SGK1*, *MXRA5*, *SOX10,* and *SLC7A5* mRNA upregulation [1]. The same tumor (GI-CCS54) was re-analyzed and confirmed to have overexpression of *MXRA5*, *SOX10,* and *SLC7A5* but not *SGK1* by qRT-PCR (Fig. 2A), suggesting a hybrid gene signature, including some genes upregulated in soft tissue CCS (*SOX10, SLC7A5*),

as well as some in AFH (*SGK1, MXRA5)* [1]. Importantly, GI-CCS lacks the melanocytic signature seen in soft tissue CCS (*PMEL, MITF*) (Fig. 2A and S1A). In contrast, SOX10 is commonly upregulated in both soft tissue CCS and GI-CCS, being strongly positive by immunohistochemistry in most cases [13, 14], suggesting that high level SOX10 expression can be used to distinguish between AFH and CCS histotypes. Interestingly, qRT-PCR performed in one GI-CCS case expressing the *EWSR1*(ex8)-*ATF1*(ex4) fusion (GI-CCS75), also showed upregulation of *SOX10, SLC7A5* and *MXRA5* and, to a lesser extent, *SGK1* and *DUSP4* (Fig. 2B and S1A), demonstrating a hybrid signature.

Whole transcriptome paired-end RNA sequencing was also performed in the subset of cases tested above, including one AFH, 2 CCS and 2 GI-CCS samples. The study group was compared to a large cohort of 186 various tumors types available on the same platform and the core gene signature for each tumor type was confirmed (Fig. S1B).

Engineered hES cells expressing the *EWSR1-CREB1* and *EWSR1-ATF1* fusions recapitulates the core transcriptional signature of human AFH and GI-CCS tumors.

The approach to generate chromosomal translocations is based on incorporation of a donor template with an hygromycin selection marker (*hyg*$^{-}$) and homology arms to guide translocation by HDR after a Cas9-induced DSB (Fig. 3A). Upon correct integration of the donor, a splice acceptor sequence (SA) allows expression of the marker (*hyg*$^{+}$) from the promoter upstream of the integration site preventing the immediate expression of the fusion transcript, which can be conditionally activated by Cre recombinase.

Reflecting the human tumor genotypes, we generated hES cell lines harboring *EWSR1* exons 1–7 fusions to *CREB1* exons 7–8 (*EWSR1*(ex7)-*CREB1*(ex7)) and either *ATF1* exons 4–7 or 5–7 (*EWSR1*(ex7)-*ATF1*(ex4) and *EWSR1*(ex7)-*ATF1*(ex5), respectively) (Fig. 3B). The *EWSR1*(ex7)-*ATF1*(ex4) fusion generates the out-of-frame transcript, which would serve as a negative control for our experiments. Hygromycin-resistant colonies were screened for correct integration of the donor at the two translocation loci by out-in, in-out PCRs, and then for the translocation using both primers outside the homology arms (out-out) (Fig. S2). At the time of transfection, cells were treated either with either DNA-PKi (NU7441) to promote HDR [11, 15, 16] or DMSO as control. For the *EWSR1*(ex7)-*CREB1*(ex7) fusion, DNA-PKi-treated plates gave 13 out of 146 *hyg*$^{+}$ clones positive for both the out-in and in-out PCRs, 2 being also positive for out-out PCR (Fig. S2). Plates treated with DMSO gave 6 out of 144 clones, although none were positive for out-out PCR, possibly due to tandem plasmid integration [11]. We also obtained 4 of 42 *hyg*$^{+}$ clones carrying *EWSR1*(ex7)-*ATF1*(ex4) and 3 of 64 *hyg*$^{+}$ clones carrying *EWSR1*(ex7)-*ATF1*(ex5), with somewhat higher efficiency using DNA-PKi (Fig. S2).

Clones harboring translocations were transfected with Cre recombinase and the resulting fusion was verified by the size change of the out-out PCR product (Fig. 3B). The reciprocal translocation (*CREB1-EWSR1* or *ATF1-EWSR1)* was confirmed by PCR and junction sequencing (Fig. 3C and S3A). Finally, these clones were examined at the targeted loci (*EWSR1* and *CREB1* or *ATF1*) in the unrearranged chromosomes of each translocation pair. Small indels within the respective introns were identified by Sanger sequencing in all but one of the clones that retained a wild-type allele (Fig. S3B). Protein expression from the

unrearranged allele was not impaired as showed by western blot analysis (Fig. S3C). Thus, these chromosomes showed no evidence of additional rearrangements.

The translocations were also tested by fluorescence in situ hybridization (FISH), using probes flanking the *EWSR1*, *CREB1* and *ATF1* genes. For the *EWSR1-CREB1* fusion, FISH showed the presence of Der22 containing the *EWSR1-CREB1* fusion, the reciprocal translocation (Der2) and, intact chromosomes 22 and 2 (Fig. 3D and S3D). The *EWSR1*(ex7)-*ATF1*(ex5) translocation and intact chromosomes 22 and 12 were also verified by FISH (Fig. S3D).

To test the induction of the transcriptional core signatures we induced the *EWSR1-CREB1* and the two *EWSR1-ATF1* fusions by Cre expression. Cells expressing Cre were enriched by cell sorting 2 days after nucleofection with the Cre-linked mCherry marker plasmid and collected at day 4 for RNA extraction. The fusion transcripts (Fig. 3E, 3F) and the chimeric protein (Fig. S3E) were identified in cells with the translocations, but not in parental or control cells. By qRT-PCR, *SGK1* and *MXRA5* was upregulated in cells expressing *EWSR1-CREB1,* while *PMEL, SOX10, SLC7A5* and *DUSP4* mRNAs were not significantly increased (Fig. 3E).

In the case of *EWSR1-ATF1* translocations, cells expressing the out-of-frame fusion *EWSR1*(ex7)-*ATF1*(ex4) showed no transcriptional changes. In contrast, cells expressing the *EWSR1*(ex7)-*ATF1*(ex5) fusion showed upregulation of *SGK1*, *MXRA5, SOX10,* and *DUSP4*, but not the melanocytic gene *PMEL* or *SLC7A5* (Fig. 3F), thus for the most part reiterating the profile of human GI-CCS. Interestingly, cells with the *EWSR1*(ex7)-*ATF1*(ex4) fusion revealed also the *EWSR1*(ex7)-*ATF1*(ex5) transcript (Fig. S3F), indicating the possibility of alternative splicing, thus recapitulating the multiple transcripts reported in human CCS tumor analysis [17, 18].

Reduced viability of hES cells upon expression of *EWSR1*(ex7)-*CREB1*(ex7) or *EWSR1*(ex7)-*ATF1*(ex5), which is not rescued by *TP53* mutation.

To study the effects of the gene fusions on viability, we performed a time course monitoring the presence of the fusions after Cre expression. For the *EWSR1-CREB1* translocation, the fusion product (with deletion of hyg^{+}) was observed at the genomic level 4 and 7 days after Cre expression (Fig. 4A, S4A), but by day 11 it returned to pre-Cre size. Concurrently, the *EWSR1-CREB1* transcript was observed at days 4 and 7 after Cre expression but was absent at day 11. These results indicate that the small population of cells that had not undergone Cre-mediated recombination had a significant growth advantage. Concurrent with the decrease in fusion transcript levels, AFH core signature genes were induced by day 4 and 7 but lost at day 11 (Fig. 4B). Thus, expression of the fusion impaired their proliferation and/or survival, enabling the overgrowth of a small population of cells not expressing the fusion. We also attempted single-cell plating to screen for fusion-expressing clones, however, none of the 5 clones recovered had undergone Cre-mediated recombination (Fig. S4B), providing evidence of *EWSR1-CREB1* fusion-associated lethality in the hES cell background.

The out-of-frame *EWSR1*(ex7)-*ATF1*(ex4) fusion was stable for 14 days after Cre expression (Fig. 4C), indicating that translocation itself is not sufficient to affect cell viability. For the in-frame *EWSR1*(ex7)-*ATF1*(ex5) translocation the recovery of mCherry-sorted cells after day 4 proved to be difficult, suggesting that the fusion was quite toxic. A time course on a pool of unsorted Cre-transfected cells showed that the fusion was detected at both genomic DNA and mRNA levels at day 2 and 6, but was absent by day 12 (Fig. 4D, Fig. S4C). The induction and decline in fusion transcript expression were accompanied by the rise and fall of the GI-CCS core gene signature (Fig. 4E). Thus, expression of the *EWSR1*(ex7)-*ATF1*(ex5) fusion in the hES cell background substantially impairs cell proliferation and/or survival.

Mutations in the tumor suppressor *TP53* are frequently detected in soft tissue sarcoma [19]. To test whether loss of TP53 would rescue cell proliferation/viability we generated null alleles of *TP53* in cells harboring the *EWSR1*(ex7)-*CREB1*(ex7) and *EWSR1*(ex7)-*ATF1*(ex5) translocations (Fig. S4D). Deletion of *TP53* did not alter the time course of expression of the fusions or the AFH gene signature, and importantly, it did not rescue the viability of hES cells (Fig. 4F, G, Fig S4E). Thus, we measured the AnnexinV 4 days after Cre-mediated fusion induction and the number of AnnexinV positive cells was increased even in $TP53^{-/-}$ cells (Fig. 4H), suggesting a TP53-independent induction of apoptosis mediated by the oncogenic fusions in hES cells.

Given the inability to propagate hES cells expressing the fusions, we asked whether these translocations could be propagated in the immortalized human embryonic kidney 293 (HEK293) that are often used for molecular studies including generation of translocations[10]. We were able to generate both translocations in HEK293 cells (Fig. S5A, B) and to recover colonies uniformly expressing both fusions with no impact on cell viability; however, these cells did not recapitulate the expression signature observed in AFH, CCS and GI-CCS tumor samples (Fig. S5A, B). Thus, HEK293 cells are not an appropriate model for these translocations.

Prolonged viability of hES-derived mesenchymal cells expressing the *EWSR1-CREB1* or *EWSR1-ATF1* fusions while maintaining the core gene signature.

Although the cell of origin of most translocation-associated sarcomas remains elusive, a potential derivation from mesenchymal stem cell progenitors has been suggested [20]. However, the use of non-immortalized mesenchymal cells to model and characterize cancer relevant chromosomal translocations has been hindered by their limited ability to be passaged [11]. Therefore, we differentiated hES cells harboring the *EWSR1-CREB1/ATF1* translocations (prior to Cre expression) to hES-derived mesenchymal progenitor (hES-MP) cells [21]. Differentiated cells were confirmed to be mesenchymal stem cells by staining for two surface markers, CD73 and CD105 (Fig. 5A). These cells were infected with a lentivirus expressing the Cre recombinase and collected at different time points to monitor fusion expression. hES-MP cells expressing the *EWSR1-CREB1* fusion remained viable longer (~1 month) compared to the hES cells, while also inducing expression of *SGK1* and *MXRA5* (Fig. 5B). Interestingly, the expression levels of *SLC7A* and *DUSP4* that were upregulated by qRT-PCR in the AFH tumors (Fig. 1E), but not in hES cells (Fig. 3E), were increased in

this cellular context. A similar observation was also seen for hES-MP cells expressing the *EWSR1-ATF1* fusion and the GI-CCS gene core signature (Fig. 5C). Thus, hES-MP cells represent a suitable system to study the *EWSR1-CREB1* and *EWSR1-ATF1* translocations and their role in cellular transformation.

EWSR1-WT1 fusion expression is associated with a distinct transcriptional signature from the *EWSR1-CREB* fusion in isogenic lines.

DSRCT is an aggressive sarcoma of presumed mesenchymal origin characterized by a t(11;22)(p13;q12) translocation, with breakpoints within the *EWSR1* and *WT1* genes (Fig. S6A) [22].

To compare with the CREB family fusions, we generated the *EWSR1* exons 1–7-*WT1* exons 8–10 (*EWSR1*(ex7)-*WT1*(ex8)) fusion in hES cells (Fig. S6B). The fusion transcript and the PCR product from the fusion were detected 2 days after Cre expression, but both were reduced over time and undetectable by day 11 (Fig. S6C).

We then induced differentiation of hES cells harboring the *EWSR1*(ex7)-*WT1*(ex8) translocation to hES-MP cells and expressed Cre recombinase. As observed with the *EWSR1-CREB1* and *EWSR1-ATF1* fusions, expression of *EWSR1-WT1* was tolerated by hES-MP cells for ~ 1 month (Fig. S6D). Importantly, in cells expressing *EWSR1-WT1* none of the genes of the AFH, CCS and GI-CCS core signatures were upregulated, while *PDGFA,* a known DSRCT target gene [23], was upregulated (Fig. S6E). Thus, these cells appear to represent a valid model to study DSRCT and provide an otherwise isogenic system to compare different *EWSR1* fusions found in distinct tumor types.

EWSR1-CREB1 fusion expression, the AFH core signature, and viability are maintained longer in a *TP53*$^{-/-}$ background.

Although the *EWSR1-CREB1* fusion is better tolerated in hES-MP cells than in hES cells, fusion expression is nevertheless reduced after several weeks. Therefore, we investigated the effect of *TP53* deletion in this cellular context by differentiating *TP53*$^{-/-}$ hES cells harboring the *EWSR1-CREB1* translocation to mesenchymal precursors (Fig. S7A). After Cre recombinase expression, we found that fusion transcripts (Fig. 6A, S7B) and the AFH core gene signature (Fig. 6B) were maintained longer (~7 weeks) with *TP53* mutation. Thus, in hES-MP cells *TP53* deletion partially rescues the lethality caused by expression of the *EWSR1-CREB1* oncogenic fusion, unlike in hES cells. We then tested if the prolonged viability resulted in anchorage-independent cell growth in a soft agar assay. Cells were plated in soft agar 3 days after infection with Cre recombinase and colony formation was monitored. Expression of the fusion was not enough to induce cellular transformation, however, colonies formed in the *TP53*$^{-/-}$ background regardless of the expression of the fusion, making it difficult to determine a specific role for fusion in this context (Fig. S7C).

To dissect the mechanism leading to extended viability in *TP53*$^{-/-}$ genetic background, gene set enrichment analysis (GSEA) was performed on whole transcriptome RNAseq comparing wild type and *TP53*$^{-/-}$ cells expressing the *EWSR1-CREB1* fusion. *TP53*$^{-/-}$ cells show downregulation of genes involved in cell cycle, apoptosis, and cellular senescence (Fig. S8A). Among these, *CDKN1A*, the gene coding for the TP53 target p21, is of

interest, because its role in cell cycle progression [24], apoptosis [25] and it is frequently downregulated in many types of cancers [26]. RT-PCR on hES-MP cells expressing the *EWSR1-CREB1* fusion confirmed the upregulation of *CDKN1A,* which is suppressed by *TP53* depletion (Fig. 6C). The level of Annexin V measured 10 and 17 days after infection was not increased in fusion expressing cells (Fig. S8B) indicating that the induction of p21 is not associated with apoptosis and suggesting that p21 may be acting instead to control cell cycle progression.

DISCUSSION

The histogenesis of translocation-associated sarcomas remains elusive, in most cases lacking a defined cell of origin [27]. Furthermore, it has become apparent that certain gene fusions are promiscuous, driving tumor pathogenesis in various cell lineages, akin to the fusions of the *EWSR1-CREB* family, which can give rise to sarcomas, carcinomas, and mesotheliomas. In this study we model *EWSR1-CREB* translocations in hES cells, an advantageous cell type for modelling oncogenic translocations, given their immortal growth, clonability, and ability to give rise to a diverse spectrum of cell types, and thus tumor types.

To reproduce the human disease, we generated *EWSR1* (exons 1–7)-*CREB1* (exons 7–8) and *EWSR1* (exons 1–7)-*ATF1* (exons 5–7) fusions commonly detected in AFH and CCS. Results showed that hES cell lines conditionally expressing the *EWSR1-CREB1* and *EWSR1-ATF1* fusions recapitulate the core transcriptional signature, respectively, of AFH and GI-CCS. However, prolonged expression of these oncogenic fusions (<12 days) impairs cell proliferation, in agreement with the embryonic lethality induced in mice expressing the *EWSR1-ATF1* fusion [28]. By contrast, HEK293 cells expressing the fusions continue to proliferate but do not recapitulate the gene signatures, likely due to the altered transcriptional output of this cell line and/or mutations in tumor suppressors oroncogenes that abrogate cell death.

While fusion induction in hES cells is sufficient to drive upregulation of genes found in AFH, CCS and GI-CCS, that by itself does not translate into cellular transformation, likely requiring additional secondary genetic events and/or epigenetic modifications, to initiate the transformation process. Based on next generation sequencing a subset of human AFH and CCS tumors is accompanied by additional mutations in tumor suppressor genes (e.g., *TP53*, *CDKN2A/B*) (MSK-IMPACT, Antonescu personal communication). Typically, *TP53* plays important roles in response to genotoxic stress and oncogene activation through cell cycle arrest, apoptosis, and senescence. However, deletion of *TP53* did not rescue cell proliferation or suppress apoptosis upon expression of either the *EWSR1-CREB1* or *EWSR1-ATF1* fusion in hES cells. A possible explanation lies in the additional role that TP53 plays in hES cells [29][30, 31] in suppressing the expression of pluripotency factors in cells under oncogenic stress and eliminating these cells by the self-renewing pool [32].

When hES cells were differentiated to mesenchymal progenitors, we found that expression of the *EWSR1-CREB1* and *EWSR1-ATF1* fusions was similarly associated with specific gene signatures of AFH and GI-CCS, but also with prolonged cell proliferation, in contrast to the rapid cell death of hES cell. Moreover, deletion of *TP53* in hES-MP cells expressing

the *EWSR1-CREB1* fusion further enhanced proliferation and/or viability, in accordance with the different role of this tumor suppressor in somatic and embryonic stem cells (Fig. 6D). TP53 exerts its tumor suppressor functions in different ways depending on the cell type, the genetic background, and the nature of the stress [33]. We provide evidence that in hES-MP cells expressing the *EWSR1-CREB1* fusion, p21, a well-known TP53 target, is upregulated. Its role in controlling cell cycle and replication speed may explain the reduced proliferation in these cells, even if other TP53-dependent or independent functions remain to be uncovered to fully rescue cell proliferation or to induce cellular transformation.

It is notable that the majority of translocation-associated sarcomas lack clear evidence of further genetic alterations, raising the possibility that epigenetic and transcriptional alterations provide an important component leading to cellular transformation. Thus, an integrated analysis of fusion positive isogenic cell lines in various differentiated backgrounds are expected to elucidate steps in cellular transformation and vulnerabilities in sarcomagenesis. Further, the approach holds promise to dissect the promiscuity observed for *EWSR1-CREB* fusions in the pathogenesis of various tumor types.

As in our work, two mouse studies have pointed to the importance of cellular background for *EWSR1-ATF1* transformation, although with seemingly contradictory results. In one model, tumors arise only when the fusion is expressed in a mesenchymal compartment [34]. In the second, however, tumors arise only in neural crest-derived peripheral nerve cells, while expression in other tissues induces senescence [35]. Thus, developing human models in different cellular contexts and differentiation stages becomes critical for resolving the issues.

In summary, our findings highlight the flexibility of the stepwise, combined approaches of CRISPR-Cas9 technology with HDR in the hES cellular context, differentiation to an appropriate cell type, and conditional fusion gene expression from the endogenous locus. More generally, this system has the potential to investigate the cell of origin in human neoplasia lacking a clear line of differentiation from phenotypic or immunohistochemical analyses, including the large group of translocation-associated sarcomas.

MATERIALS AND METHODS

Mammalian cell culture.

All experiments were approved by the Tri-SCI Embryonic Stem Cell Research Oversight Committee (ESCRO). Human embryonic stem cells (WA01, H1) were cultured in E8 medium (Life technologies, #A1517001) on vitronectin-coated plates (Life technologies, #A14700). HEK293 cells were cultured in DME-HG with 10% fetal bovine serum. hES-MP cells were generated and maintained following the manufacturer’s instructions (STEMCELL Technologies, #05240).

Tumor Samples.

Human samples were collected from consenting patients (Institutional Review Board 02–060).

Gene expression and whole transcriptome sequencing.

Affymetrix U133A was performed comparing 3 AFH, 4 CCS cases, to a group of 44 tumors of various histotypes and 6 normal tissues, using log2-fold change threshold of 1, FDR 0.01 [36, 37]. Total RNA was extracted using RNeasy Plus Mini (Qiagen) and prepared for RNA sequencing following Illumina protocol [38]. All reads were aligned with STAR (ver 2.3) and BowTie2 against the human reference genome (hg19). The mRNA expression of the genes in the core signatures of AFH, CCS, and GI-CCS [1] was investigated on the 5 study group samples and 186 of various tumor types. Pathway enrichment analyses were performed using online curated gene set, gene ontology and transcription factors binding site collections on the Gene Set Enrichment Analysis software (http://software.broadinstitute.org/gsea/msigdb/index.jsp). Data are available at https://www.ncbi.nlm.nih.gov/geo/query/acc.cgi?acc=GSE168562.

Generation of cell lines.

Cells were transfected by Amaxa nucleofector with 2.5 μg of each plasmid (gRNAs and donor plasmid), plated and treated with 0.1μM DNA-PKcs inhibitor (NU7441) or DMSO for 24 h, before selection with 150 μg/ml hygromycin. Hygromycin-resistant colonies were picked in 96-well plate for PCR analysis. *TP53* knockout clones were generated by nucleofection of a vector expressing *TP53* gRNA [39] and confirmed by western blot.

Generation of plasmids.

Donors were obtained from plasmid previously described [11]. Homology arms (HAs) were amplified from hES cells and cloned at NotI-NheI (*EWSR1*) or SalI-ApaI (*CREB1*, *ATF1* and *WT1*) cloning sites. gRNAs were cloned into pSpCas9(BB)-2A-Puro (PX459, Addgene 48139) as previously described [40]. Primers and oligos are listed in Tables S1 and S2.

PCR analysis.

PCRs were performed using Jeffrey's Buffer PCR buffer with Taq Polymerase [41] under condition previously described [40]. The primers, the annealing temperature (T_a) and extension time for each reaction are listed in Table S3.

RT-PCR.

cDNA was synthesized by SuperScript IV First-Strand Synthesis System (Invitrogen, #18091050). RT-PCR conditions were previously described [11] qRT-PCR was done on QuantStudio 3Real-Time PCR system with Powerup SYBER green master mix (Applied Biosystem, #A25743). Quantification was performed with $\Delta\Delta C_t$ method using *GAPDH* as standard. No-template reactions were performed as negative controls. Primers used for RT-PCR and qRT-PCR are listed in Tables S4 and S5.

Flow cytometry.

Staining for surface markers was done as previously described [11] with antibodies listed in Table S6. Acquisition was done using a Becton Dickinson FACScan and the analysis by FlowJo software.

Cre Expression.

hES cells were transfected with 3 μg of a plasmid expressing Cre and mCherry marker [11] and harvested 48 h after for enrichment by FACS of mCherry-positive cells. hES-MP were infected with a self-deleting lentivirus expressing Cre [42]. Cells were collected for DNA and RNA extraction.

Apoptosis assay.

Cells were collected 4 days after transfection (hES) or 10 and 17 days after infection (hES-MP) with Cre and labeled using FITC AnnexinV kit (Biolegend, 640905) according to manufacturer's instruction and propidium iodide, followed by flow cytometry and quantification by FlowJo software.

Cell Transformation assay.

Cell Transformation Assay Kit (ab235698) was performed as instructed by manufacturer. Briefly, 4 day after Cre-infection hES-MP cells were resuspended in 75μL of DMEM 10% FBS mixed with 0.3% (wt/vol) agarose and added to 96-well plate pre-coated with 75μL media mixed with 0.6% (wt/vol) agarose (10,000 cells/well).

Western Blot.

Cell lysate was prepared as previously described [11] and separated on 4–12% Bis-Tris Protein gel. After transfer and blocking in PBS 5% (wt/vol) milk, nitrocellulose membrane was probed over-night with primary antibodies (Table S6) and incubated with secondary antibody for 1 h. Proteins were visualized with Plus-ECL Enhanced Chemiluminescence.

Fluorescence in situ hybridizatio.

Custom BAC probes (Table S7) for *EWSR1*, *CREB1* and *ATF1* were applied on slides with metaphase spreads, using standard protocol [43]. Metaphases were imaged using the metasystem (Zeiss Imager.2 and ISIS 5.2) (Metasystems, Boston, USA).

Statistical analysis.

Analysis was performed using the Graphpad software. Number of experiments is indicated in figure legends. Numerical data are shown as the mean±s.d and differences between groups were determined using paired or unpaired t-test. p-value <0.05 was considered statistically significant. If not specified, the analysis is not significant.

Supplementary Material

Refer to Web version on PubMed Central for supplementary material.

Acknowledgments.

We thank Chew-Li Soh and Xian Zhang for technical assistance and reagents; members of the Jasin Laboratory for discussions and suggestions; and Rohit Prakash, Travis White and Pei Xin Lim for critical reading of the manuscript. This work was supported in part by: R35 CA253174 (MJ), P50 CA140146 (CRA), P50 CA217694 (CRA), Cycle for Survival (CRA), Kristin Ann Carr Foundation (CRA), St Baldrick Foundation (CRA). Core facilities at MSK are supported by the Cancer Center Support Grant (NIH P30 CA008748).

REFERENCES

1. Antonescu CR, Dal Cin P, Nafa K, Teot LA, Surti U, Fletcher CDet al.EWSR1-CREB1 is the predominant gene fusion in angiomatoid fibrous histiocytoma. Genes Chromosomes Cancer.2007; 46: 1051–1060. [PubMed: 17724745]
2. Antonescu CR, Tschernyavsky SJ, Woodruff JM, Jungbluth AA, Brennan MF, Ladanyi M. Molecular diagnosis of clear cell sarcoma: detection of EWS-ATF1 and MITF-M transcripts and histopathological and ultrastructural analysis of 12 cases. The Journal of molecular diagnostics : JMD.2002; 4: 44–52. [PubMed: 11826187]
3. Antonescu CR, Nafa K, Segal NH, Dal Cin P, Ladanyi M. EWS-CREB1: a recurrent variant fusion in clear cell sarcoma--association with gastrointestinal location and absence of melanocytic differentiation. Clin Cancer Res.2006; 12: 5356–5362. [PubMed: 17000668]
4. Thway K, Nicholson AG, Lawson K, Gonzalez D, Rice A, Balzer Bet al.Primary pulmonary myxoid sarcoma with EWSR1-CREB1 fusion: a new tumor entity. Am J Surg Pathol.2011; 35: 1722–1732. [PubMed: 21997693]
5. Desmeules P, Joubert P, Zhang L, Al-Ahmadie HA, Fletcher CD, Vakiani Eet al.A Subset of Malignant Mesotheliomas in Young Adults Are Associated With Recurrent EWSR1/FUS-ATF1 Fusions. Am J Surg Pathol.2017; 41: 980–988. [PubMed: 28505004]
6. Antonescu CR, Katabi N, Zhang L, Sung YS, Seethala RR, Jordan RCet al.EWSR1-ATF1 fusion is a novel and consistent finding in hyalinizing clear-cell carcinoma of salivary gland. Genes Chromosomes Cancer.2011; 50: 559–570. [PubMed: 21484932]
7. Rossi S, Szuhai K, Ijszenga M, Tanke HJ, Zanatta L, Sciot Ret al.EWSR1-CREB1 and EWSR1-ATF1 fusion genes in angiomatoid fibrous histiocytoma. Clin Cancer Res.2007; 13: 7322–7328. [PubMed: 18094413]
8. Wang WL, Mayordomo E, Zhang W, Hernandez VS, Tuvin D, Garcia Let al.Detection and characterization of EWSR1/ATF1 and EWSR1/CREB1 chimeric transcripts in clear cell sarcoma (melanoma of soft parts). Mod Pathol.2009; 22: 1201–1209. [PubMed: 19561568]
9. Braunreiter CL, Hancock JD, Coffin CM, Boucher KM, Lessnick SL. Expression of EWS-ETS fusions in NIH3T3 cells reveals significant differences to Ewing's sarcoma. Cell cycle.2006; 5: 2753–2759. [PubMed: 17172842]
10. Brunet E, Jasin M. Induction of Chromosomal Translocations with CRISPR-Cas9 and Other Nucleases: Understanding the Repair Mechanisms That Give Rise to Translocations. Advances in experimental medicine and biology.2018; 1044: 15–25. [PubMed: 29956288]
11. Vanoli F, Tomishima M, Feng W, Lamribet K, Babin L, Brunet Eet al.CRISPR-Cas9-guided oncogenic chromosomal translocations with conditional fusion protein expression in human mesenchymal cells. Proc Natl Acad Sci U S A.2017; 114: 3696–3701. [PubMed: 28325870]
12. Hisaoka M, Ishida T, Kuo TT, Matsuyama A, Imamura T, Nishida Ket al.Clear cell sarcoma of soft tissue: a clinicopathologic, immunohistochemical, and molecular analysis of 33 cases. Am J Surg Pathol.2008; 32: 452–460. [PubMed: 18300804]
13. Stockman DL, Miettinen M, Suster S, Spagnolo D, Dominguez-Malagon H, Hornick JLet al.Malignant gastrointestinal neuroectodermal tumor: clinicopathologic, immunohistochemical, ultrastructural, and molecular analysis of 16 cases with a reappraisal of clear cell sarcoma-like tumors of the gastrointestinal tract. Am J Surg Pathol.2012; 36: 857–868. [PubMed: 22592145]
14. Karamchandani JR, Nielsen TO, van de Rijn M, West RB. Sox10 and S100 in the diagnosis of soft-tissue neoplasms. Applied immunohistochemistry & molecular morphology : AIMM / official publication of the Society for Applied Immunohistochemistry.2012; 20: 445–450.
15. Pierce AJ, Hu P, Han M, Ellis N, Jasin M. Ku DNA end-binding protein modulates homologous repair of double-strand breaks in mammalian cells. Genes & development.2001; 15: 3237–3242. [PubMed: 11751629]
16. Vriend LE, Prakash R, Chen CC, Vanoli F, Cavallo F, Zhang Yet al.Distinct genetic control of homologous recombination repair of Cas9-induced double-strand breaks, nicks and paired nicks. Nucleic acids research.2016; 44: 5204–5217. [PubMed: 27001513]

17. Jakubauskas A, Valceckiene V, Andrekute K, Seinin D, Kanopka A, Griskevicius L. Discovery of two novel EWSR1/ATF1 transcripts in four chimerical transcripts-expressing clear cell sarcoma and their quantitative evaluation. Exp Mol Pathol.2011; 90: 194–200. [PubMed: 21185830]
18. Panagopoulos I, Mertens F, Debiec-Rychter M, Isaksson M, Limon J, Kardas Iet al.Molecular genetic characterization of the EWS/ATF1 fusion gene in clear cell sarcoma of tendons and aponeuroses. Int J Cancer.2002; 99: 560–567. [PubMed: 11992546]
19. Toguchida J, Yamaguchi T, Ritchie B, Beauchamp RL, Dayton SH, Herrera GEet al.Mutation spectrum of the p53 gene in bone and soft tissue sarcomas. Cancer Res.1992; 52: 6194–6199. [PubMed: 1423262]
20. Tirode F, Laud-Duval K, Prieur A, Delorme B, Charbord P, Delattre O. Mesenchymal stem cell features of Ewing tumors. Cancer cell.2007; 11: 421–429. [PubMed: 17482132]
21. Liang Q, Monetti C, Shutova MV, Neely EJ, Hacibekiroglu S, Yang Het al.Linking a cell-division gene and a suicide gene to define and improve cell therapy safety. Nature.2018; 563: 701–704. [PubMed: 30429614]
22. Gerald WL, Rosai J, Ladanyi M. Characterization of the genomic breakpoint and chimeric transcripts in the EWS-WT1 gene fusion of desmoplastic small round cell tumor. Proc Natl Acad Sci U S A.1995; 92: 1028–1032. [PubMed: 7862627]
23. Lee SB, Kolquist KA, Nichols K, Englert C, Maheswaran S, Ladanyi Met al.The EWS-WT1 translocation product induces PDGFA in desmoplastic small round-cell tumour. Nat Genet.1997; 17: 309–313. [PubMed: 9354795]
24. Bertoli C, Skotheim JM, de Bruin RA. Control of cell cycle transcription during G1 and S phases. Nature reviews Molecular cell biology.2013; 14: 518–528. [PubMed: 23877564]
25. Gartel AL, Tyner AL. The role of the cyclin-dependent kinase inhibitor p21 in apoptosis. Mol Cancer Ther.2002; 1: 639–649. [PubMed: 12479224]
26. Abbas T, Dutta A. p21 in cancer: intricate networks and multiple activities. Nat Rev Cancer.2009; 9: 400–414. [PubMed: 19440234]
27. Mertens F, Antonescu CR, Mitelman F. Gene fusions in soft tissue tumors: Recurrent and overlapping pathogenetic themes. Genes Chromosomes Cancer.2016; 55: 291–310. [PubMed: 26684580]
28. Haldar M, Hancock JD, Coffin CM, Lessnick SL, Capecchi MR. A conditional mouse model of synovial sarcoma: insights into a myogenic origin. Cancer cell.2007; 11: 375–388. [PubMed: 17418413]
29. Qin H, Yu T, Qing T, Liu Y, Zhao Y, Cai Jet al.Regulation of apoptosis and differentiation by p53 in human embryonic stem cells. J Biol Chem.2007; 282: 5842–5852. [PubMed: 17179143]
30. Filion TM, Qiao M, Ghule PN, Mandeville M, van Wijnen AJ, Stein JLet al.Survival responses of human embryonic stem cells to DNA damage. J Cell Physiol.2009; 220: 586–592. [PubMed: 19373864]
31. Aladjem MI, Spike BT, Rodewald LW, Hope TJ, Klemm M, Jaenisch Ret al.ES cells do not activate p53-dependent stress responses and undergo p53-independent apoptosis in response to DNA damage. Curr Biol.1998; 8: 145–155. [PubMed: 9443911]
32. Lin T, Chao C, Saito S, Mazur SJ, Murphy ME, Appella Eet al.p53 induces differentiation of mouse embryonic stem cells by suppressing Nanog expression. Nature cell biology.2005; 7: 165–171. [PubMed: 15619621]
33. Zilfou JT, Lowe SW. Tumor suppressive functions of p53. Cold Spring Harb Perspect Biol.2009; 1: a001883. [PubMed: 20066118]
34. Straessler KM, Jones KB, Hu H, Jin H, van de Rijn M, Capecchi MR. Modeling clear cell sarcomagenesis in the mouse: cell of origin differentiation state impacts tumor characteristics. Cancer cell.2013; 23: 215–227. [PubMed: 23410975]
35. Komura S, Ito K, Ohta S, Ukai T, Kabata M, Itakura Fet al.Cell-type dependent enhancer binding of the EWS/ATF1 fusion gene in clear cell sarcomas. Nature communications.2019; 10: 3999.
36. Hajdu M, Singer S, Maki RG, Schwartz GK, Keohan ML, Antonescu CR. IGF2 over-expression in solitary fibrous tumours is independent of anatomical location and is related to loss of imprinting. J Pathol.2010; 221: 300–307. [PubMed: 20527023]

37. Antonescu CR, Yoshida A, Guo T, Chang NE, Zhang L, Agaram NPet al.KDR activating mutations in human angiosarcomas are sensitive to specific kinase inhibitors. Cancer Res.2009; 69: 7175–7179. [PubMed: 19723655]

38. Antonescu CR, Le Loarer F, Mosquera JM, Sboner A, Zhang L, Chen CLet al.Novel YAP1-TFE3 fusion defines a distinct subset of epithelioid hemangioendothelioma. Genes Chromosomes Cancer.2013; 52: 775–784. [PubMed: 23737213]

39. Feng W, Jasin M. BRCA2 suppresses replication stress-induced mitotic and G1 abnormalities through homologous recombination. Nature communications.2017; 8: 525.

40. Vanoli F, Jasin M. Generation of chromosomal translocations that lead to conditional fusion protein expression using CRISPR-Cas9 and homology-directed repair. Methods.2017; 121–122: 138–145.

41. Zhang Y, Vanoli F, LaRocque JR, Krawczyk PM, Jasin M. Biallelic targeting of expressed genes in mouse embryonic stem cells using the Cas9 system. Methods.2014; 69: 171–178. [PubMed: 24929070]

42. Pfeifer A, Brandon EP, Kootstra N, Gage FH, Verma IM. Delivery of the Cre recombinase by a self-deleting lentiviral vector: efficient gene targeting in vivo. Proc Natl Acad Sci U S A.2001; 98: 11450–11455. [PubMed: 11553794]

43. Kao YC, Sung YS, Zhang L, Chen CL, Vaiyapuri S, Rosenblum MKet al.EWSR1 Fusions With CREB Family Transcription Factors Define a Novel Myxoid Mesenchymal Tumor With Predilection for Intracranial Location. Am J Surg Pathol.2017; 41: 482–490. [PubMed: 28009602]

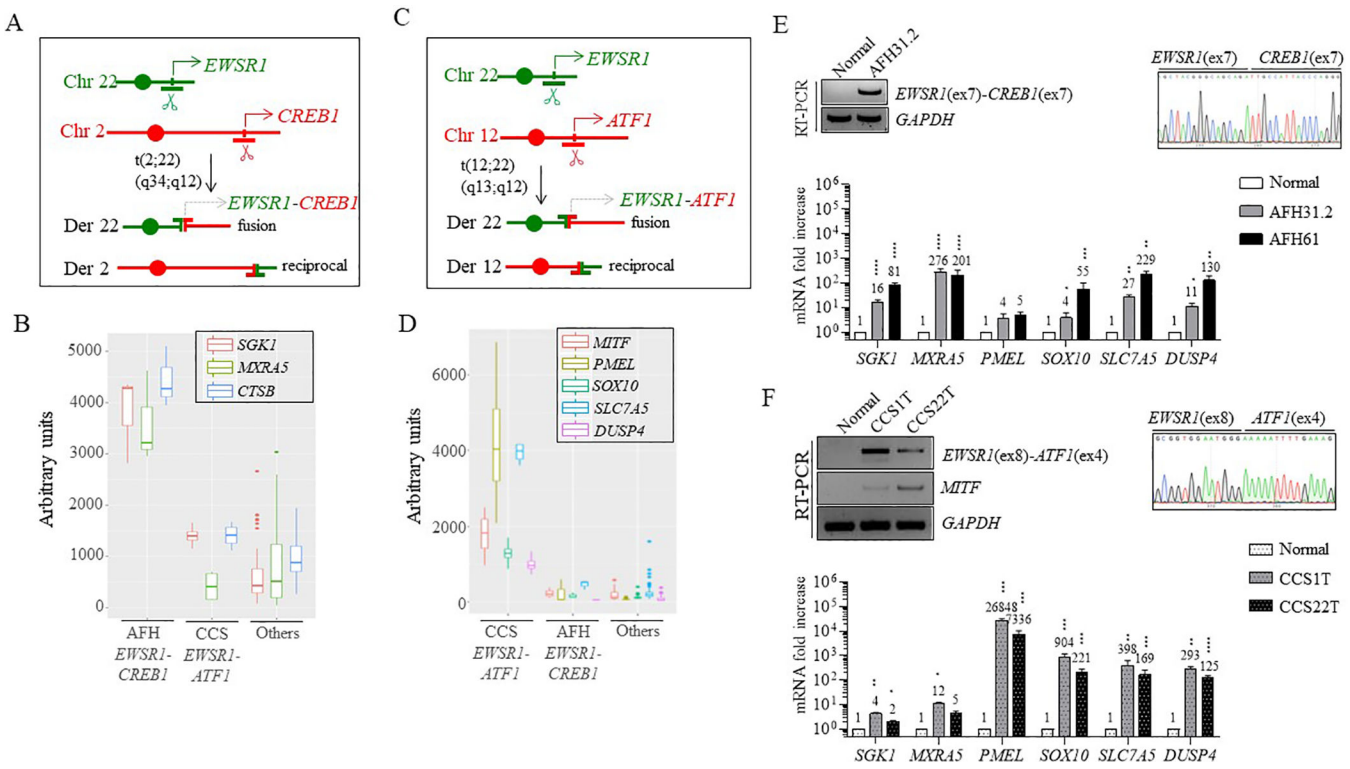

Figure 1. Gene expression signatures of human AFH and CCS.

(A) AFH is associated with the t(2;22)(q34;q12) translocation, resulting in an *EWSR1-CREB1* fusion.

(B)*EWSR1-CREB1* fusion-positive AFH tumors have high transcript levels of *SGK1*, *MXRA5*, and *CTSB* (3 cases), as compared to CCS tumors (4 cases), 44 other sarcomas (5 angiosarcoma AS, 3 fibrosarcoma FS, 5 gastrointestinal stromal tumors GIST, 11 paraganglioma CTR, 3 leiomyosarcoma LMS, 3 myxoid liposarcoma MLS, 3 undifferentiated pleomorphic sarcoma MFH, 3 synovial sarcoma SS, 4 solitary fibrous tumor SFT, 4 small blue round cell tumor SBRCT) and 6 normal tissues (testis, brain, adrenal, kidney, small intestine and fetal stomach), (“Others”).

(C) CCS is associated with t(12;22)(q13;q12) translocation, resulting in an *EWSR1-ATF1* gene fusion. **(D)** *EWSR1-ATF1* fusion-positive CCS tumors (4 cases) have high transcript levels of several genes, in particular, *PMEL* and *SLC7A5*, as compared to AFH tumors and other sarcomas and normal tissues (same as in panel B).

(E) Two additional *EWSR1-CREB1* fusion-positive AFH (AFH31.2 and AFH61) samples show high mRNA levels of *SGK1*, *MXRA5*, *SLC7A5* and *DUSP4* and to a lesser extent, *SOX10*, as compared with normal tissue. *CTSB* is also high in these two tumors, but it is not present in normal tissue. RT-PCR and Sanger sequencing showing the *EWSR1*(ex7)-*CREB1*(ex7) fusion in AFH31.2 is also included.

(F) Two additional *EWSR1-ATF1* fusion-positive CCS (1T and 22T) cases revealed similarly high levels of expression in the genes shown in (D). RT-PCR and Sanger sequencing showing the in frame *EWSR1*(ex8)-*ATF1*(ex4) fusion and *MITF* expression in these two tumors, but not in normal tissue.

Numerical values indicate fold increase compared to normal tissue. Error bars in this figure represent standard deviation from the mean of at least three technical replicates. Statistical significance is calculated by comparison of tumor samples with normal tissue. *p<0.05; **p<0.01; ***p<0.001; ****p<0.0001 (paired t-test).

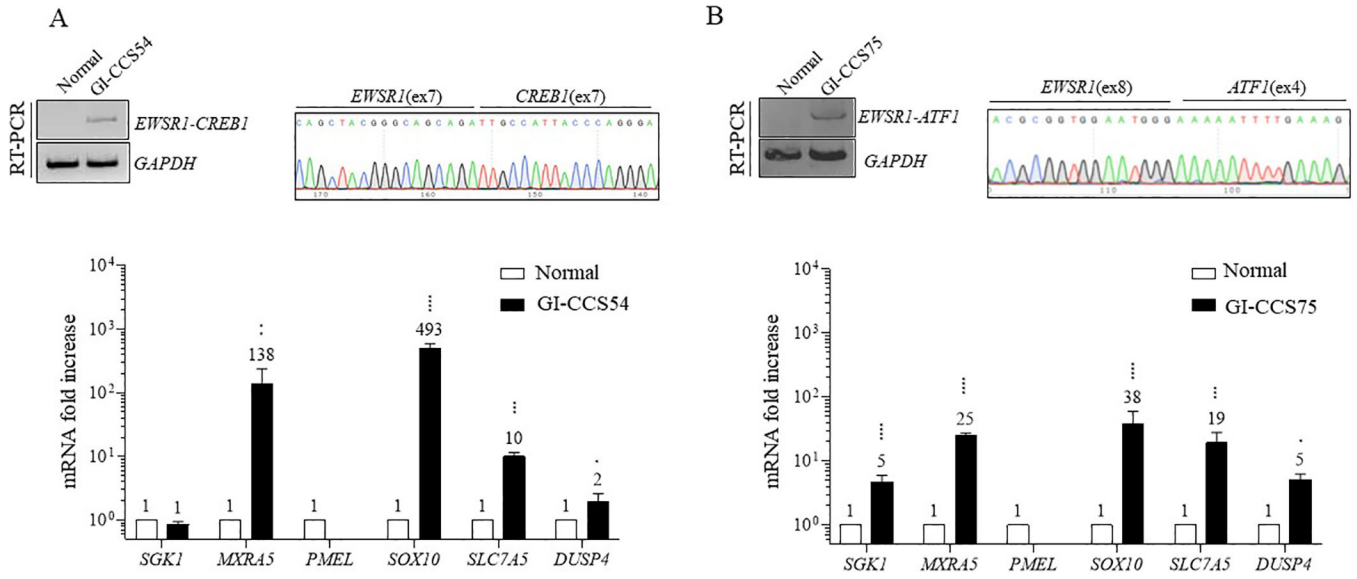

Figure 2. Gene expression signature of GI-CCS tumors expressing *EWSR1-CREB1* and *EWSR1-ATF1* fusions.

(A) An *EWSR1-CREB1* fusion-positive GI-CCS (GI-CCS54) demonstrates upregulation of *MXRA5, SOX10* and *SLC7A5,* and to lesser extent *DUSP4*, but not *SGK1*. RT-PCR and Sanger sequencing show the in-frame *EWSR1*(ex7)-*CREB1*(ex7) fusion.

(B) An *EWSR1-ATF1* fusion-positive GI-CCS (GI-CCS75) also demonstrates high levels of the genes shown in (A), as well as *SGK1*. RT-PCR and Sanger sequencing show the in-frame *EWSR1*(ex8)-*ATF1*(ex4) fusion. Numerical values indicate fold increase compared to normal tissue. Statistical analysis same as in Fig. 1. Fold increase values for *PMEL* are ≤1 (0.074 and 0.17 respectively).

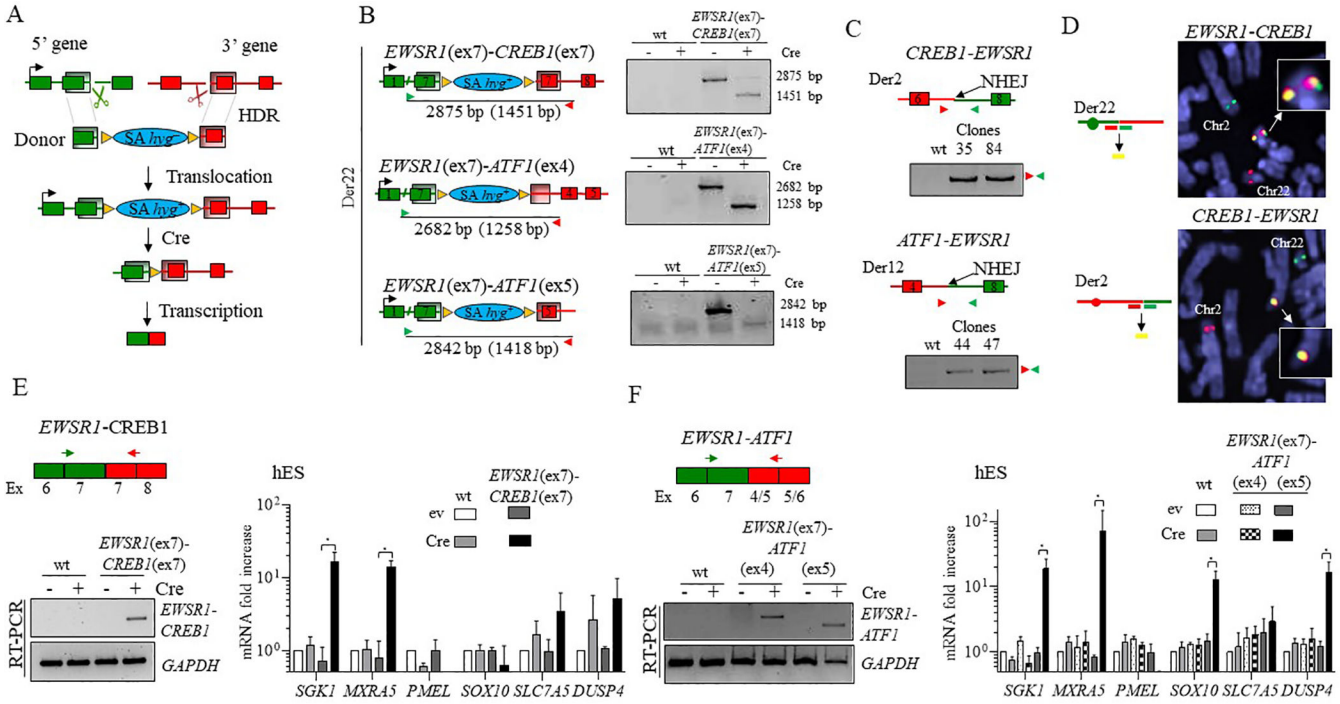

Figure 3. Generation and expression of *EWSR1-CREB1* and *EWSR1-ATF1* fusions in hES cells.

(A) Chromosomal translocation strategy for conditional fusion gene expression. A donor template containing a promoter-less selectable marker hygromycin (*hyg*$^{-}$) and two homology arms (shaded regions) is inserted by HDR at the gRNA-mediated DSBs (scissors) at the chromosomal locations of the 5' and 3' fusion partners. An in-frame splice acceptor (SA) sequence upstream of *hyg*$^{-}$ allows expression of the gene upon correct integration of the donor (*hyg*$^{+}$), allowing selection in hygromycin. Transcription of the fusion gene is dependent on removal of the selectable marker by Cre recombinase.

(B) Fusion genes are formed upon Cre expression. Left, Schematic representation of the three translocations prior to Cre expression, with the size of the PCR products across the breakpoint junctions before and after (in parenthesis) removal of *hyg*$^{+}$. Right, a PCR size shift confirms the formation of the direct fusion for each of the translocations.

(C) The reciprocal translocations confirmed by PCR analysis in the clones harboring the *EWSR1*(ex7)-*CREB1*(ex7) and *EWSR1*(ex7)-*ATF1*(ex5) translocations.

(D) Dual color FISH analysis showing the *EWSR1* and *CREB1* loci and the resulting derivative chromosomes, Der 22 (top) and Der 2 (bottom), using the indicated "split" probes (i.e., two for each gene). Note that in the top image, the *EWSR1* and *CREB1* probes do not match the chromosome coloring scheme). Unrearranged chromosomes 2 and 22 are also indicated.

(E) Induction of the *EWSR1*(ex7)-*CREB1*(ex7) fusion after Cre expression in hES cells results in upregulation of *SGK1* and *MXRA5* (ev, empty vector). Histogram represents the mean fold increase compared to empty vector condition of wild type cells as measured by $\Delta\Delta C_t$ method and error bars indicate the standard deviation from the mean of 3 independent experiments. Statistical significance is calculated with a paired t-test comparing Cre

condition with the corresponding control (ev). *p<0.05; when not indicated, the difference is considered not statistically significant.

(F) Induction of the *EWSR1*(ex7)-*ATF1*(ex5) fusion, but not the *EWSR1*(ex7)-*ATF1*(ex4), after Cre expression in hES cells results in upregulation of GI-CCS core signature genes, *SGK1*, *MXRA5*, *SOX10,* and *DUSP4* (ev, empty vector). Statistical analysis as in panel E, n=3.

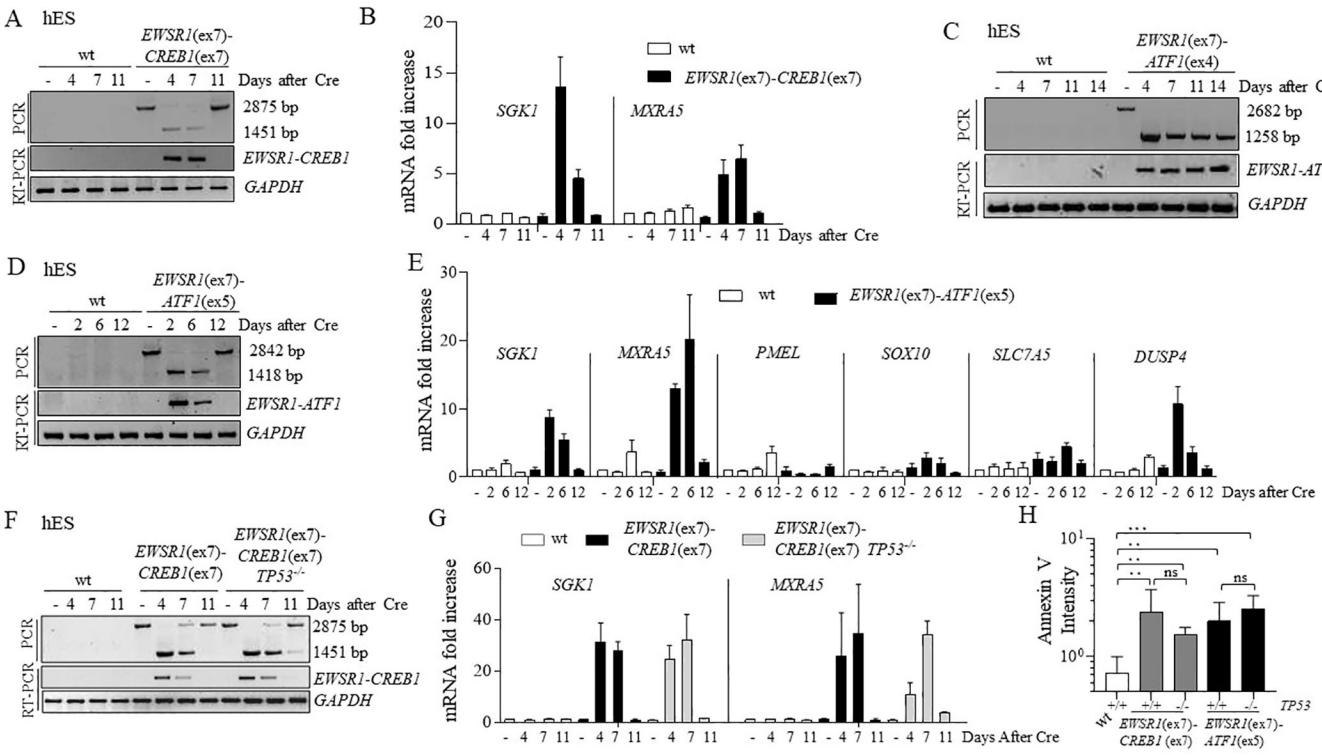

Figure 4. Impaired proliferation of hES cells upon *EWSR1*(ex7)-*CREB1*(ex7) or *EWSR1*(ex7)-*ATF1*(ex5) fusion expression.

(A) Time course of the *EWSR1*(ex7)-*CREB1*(ex7) fusion after Cre expression. The fusion was analyzed using both PCR of genomic DNA and RT-PCR. The lower band in the PCR is the direct fusion, while the upper band indicates that the fusion partners are separated by the *hyg*$^{+}$ gene. See Fig. 3B.

(B) Time course for expression of AFH signature genes *SGK1* and *MXRA5* using qRT-PCR upon *EWSR1*(ex7)-*CREB1*(ex7) fusion in sorted cells. Histogram represents the fold increase compared to wild type cells (-Cre condition) of 1 representative experiment (n=3).

(C) Same as panel A for the *EWSR1*(ex7)-*ATF1*(ex4) fusion.

(D) Same as panel A for the *EWSR1*(ex7)-*ATF1*(ex5) fusion.

(E) Time course for expression analysis using qRT-PCR upon *EWSR1*(ex7)-*ATF1*(ex5) fusion in pooled cells. Histogram represents the mean of fold increase compared to wild type cells (-Cre conditions) of 2 independent experiments.

(F) Same as panel A for the *EWSR1*(ex7)-*CREB1*(ex7) fusion with, in addition, *TP53*$^{-/-}$ cells.

(G) Time course for expression of AFH signature genes using qRT-PCR upon *EWSR1*(ex7)-*CREB1*(ex7) fusion induction in wild-type and *TP53*$^{-/-}$ background. Histogram represents the fold increase to wild type of 1 representative experiment (n=3).

(H) Quantification of Annexin V staining for measurement of apoptosis. Annexin V intensity is represented as the ratio of the percentages of Cre and empty vector-transfected cells. Error bars represent standard deviation from the mean of n≥3 independent experiments. Unpaired t-test, *p<0.05, **p<0.01, ***p<0.001, ns=not significant.

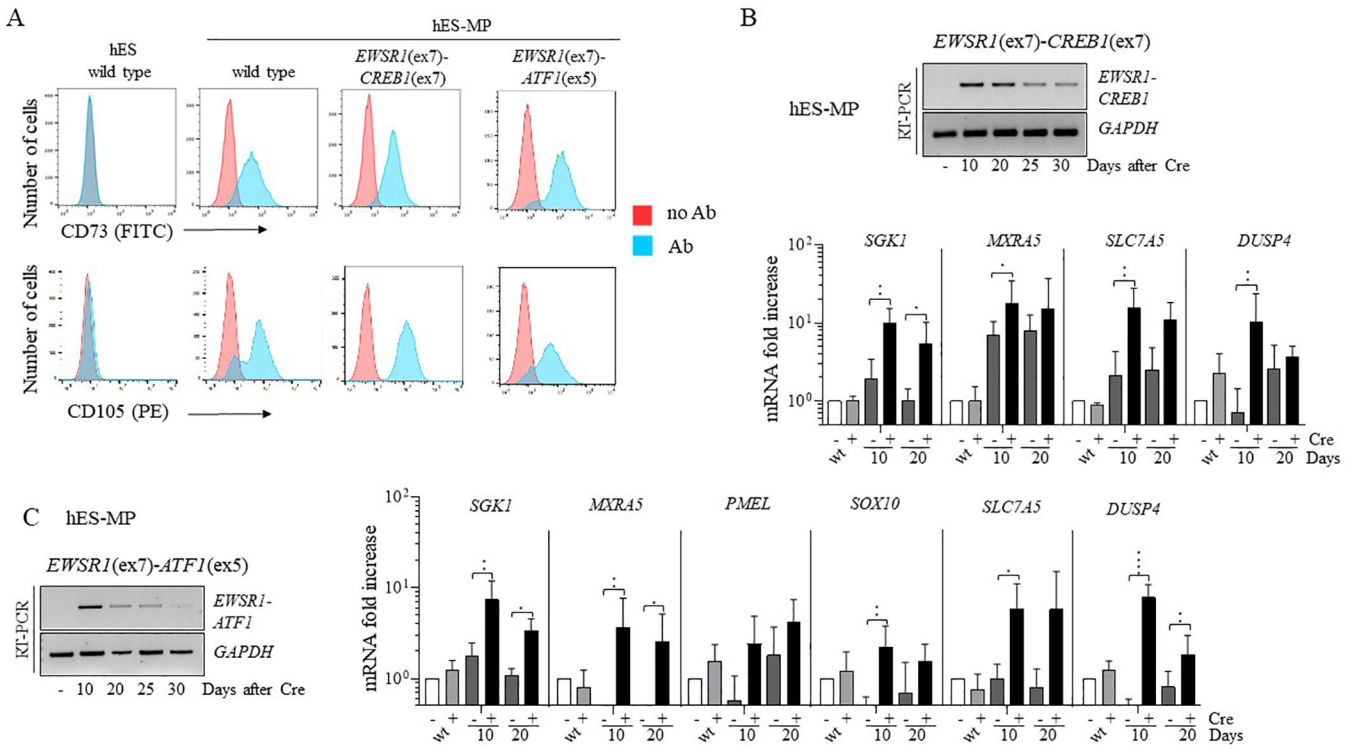

Figure 5. Viability of hES-derived mesenchymal cells expressing *EWSR1-CREB1* and *EWSR1-ATF1* while maintaining the AFH and CCS core gene signatures.

(A) hES-MP cells express mesenchymal surface markers CD73 and CD105. *EWSR1*(ex7)-*CREB1*(ex7) and *EWSR1*(ex7)-*ATF1*(ex5) refer to cells carrying the translocation prior to Cre expression.

(B) Time course in days of *EWSR1-CREB1* fusion expression in hES-MP cells after Cre expression. The AFH core gene signature is detected in hES-MP cells expressing the *EWSR1*(ex7)-*CREB1*(ex7) fusion over time. Histogram represents the fold increase compared to wild type cells (-Cre condition) and the error bars the standard deviation from the mean of 4 independent experiments. Statistical significance is calculated with a paired t-test comparing +Cre with the corresponding -Cre condition. *p<0.05, **p<0.01; when not indicated the difference is considered not statistically significant.

(C) Same as panel B for the *EWSR1*(ex7)-*ATF1*(ex5) fusion. qRT-PCR in hES-MP cells expressing the *EWSR1*(ex7)-*ATF1*(ex5) at different time points. Statistical analysis as in panel B, n=5. *p<0.05, **p<0.01, ***p<0.001, ****p<0.0001.

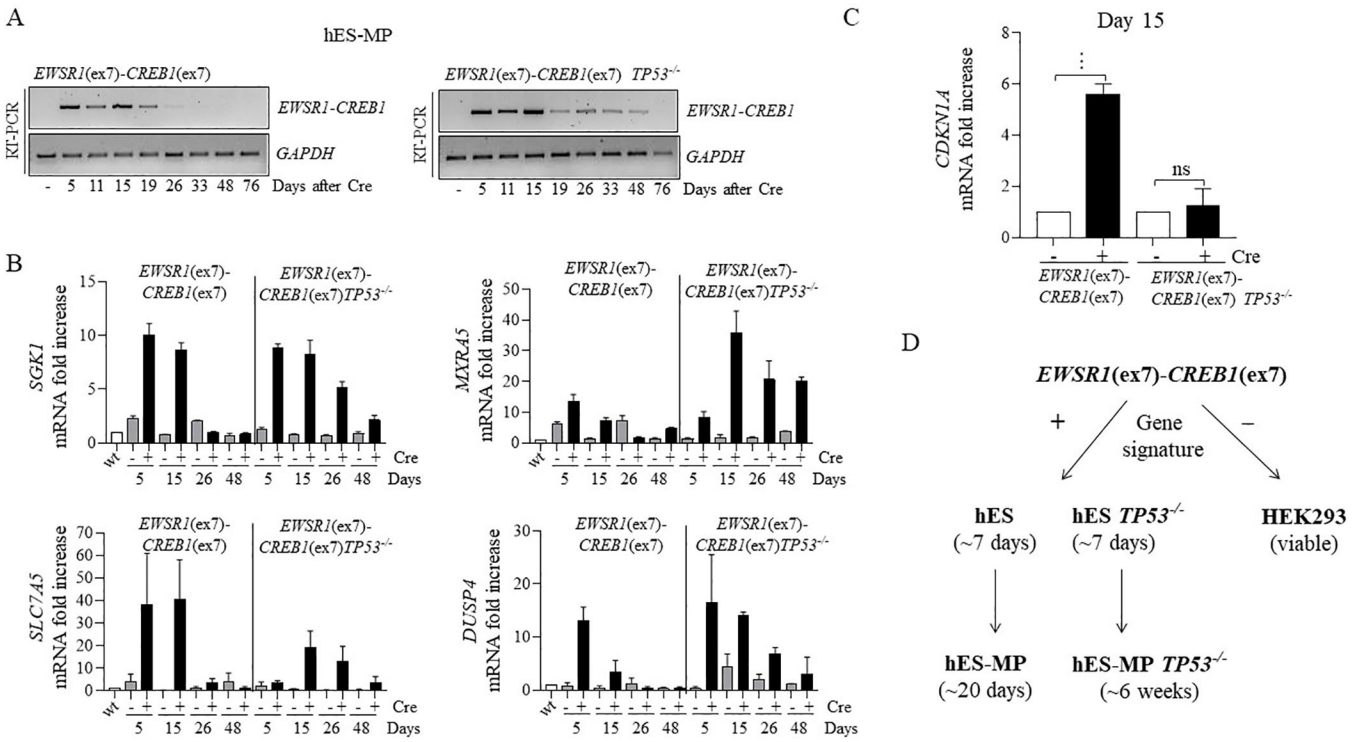

Figure 6. Prolonged viability of hES-derived mesenchymal cells expressing *EWSR1-CREB1* in *TP53*$^{-/-}$ background.

(A) Time course in days for *EWSR1-CREB1* fusion expression and **(B)** AFH core gene signature in wild type and *TP53*$^{-/-}$ genetic background. Histogram represents the fold increase to wild type (-Cre condition) of 1 representative experiment (n=2). **(C)** *CDKN1A* expression is measured 15 days after the induction of the *EWSR1-CREB1* fusion in wild type and *TP53*$^{-/-}$ cells. Histogram represents the fold increase of the +Cre condition compared to the corresponding -Cre condition and the error bars the standard deviation from the mean of 3 independent experiments. Statistical significance is calculated with a paired t-test comparing the +Cre with the corresponding -Cre condition. ***p<0.001, ns=not significant. **(D)** *EWSR1*(ex7)-*CREB1*(ex7) fusion expression impairs the cell proliferation/viability of hES cell after 7 days, regardless of *TP53* deletion. On the contrary, in hES-MP the viability is prolonged and is further expanded by deletion of *TP53* (see discussion for details).